

Computation of transport coefficients and the dynamical structure factor of Xe in the presence of long-range three-body interactions

D. Levesque and J. J. Weis

Laboratoire de Physique Théorique et Hautes Energies, Université de Paris XI, Bâtiment 211, 91405 Orsay Cédex, France

J. Vermesse

Laboratoire des Interactions Moléculaires et des Hautes Pressions, Centre Universitaire de Paris-Nord, Avenue J. B. Clément, 93430 Villetaneuse, France

(Received 2 June 1987)

The importance of the three-body dispersion interaction (Axilrod-Teller potential) in liquid Xe near its triple point is investigated by numerical simulations. Although large for the heavy rare gas Xe, its effect on collective dynamical properties such as the dynamical structure factor and transport coefficients is very small. When used in conjunction with an accurate pair potential, good agreement is obtained with experiment for both the pressure and transport coefficients.

I. INTRODUCTION

Pair potentials which accurately reproduce the low-density thermodynamic and transport properties are now known for most rare gases so that one can legitimately address the question of the importance of many-body interactions. It has been known since the work of Barker and collaborators¹ and has been emphasized again quite recently²⁻⁴ that the use of an accurate pair potential together with the three-body Axilrod-Teller (AT) triple-dipole interaction—though valid only for large separations of the atoms—gives a remarkably faithful representation of the cohesive energies of rare-gas crystals at 0 K (Ref. 4) and of the equation of state of the liquid and solid phases up to pressures of about 20 kbar.^{2,3} At the same time it has been recognized that short-range three-body forces (e.g., first-order three-body exchange interactions) give contributions comparable in magnitude with the AT interaction⁴⁻⁷ and of opposite sign so that the good agreement with experiment obtained with the AT potential has either to be considered as fortuitous or to be attributed to substantial cancellation between non-AT many-body interactions.

There is, however, also evidence for situations in which a pair plus AT potential description does not well reproduce experimental results. These include the equation of state for rare-gas solids at very high pressures,⁸⁻¹⁰ rare-gas cluster stability,¹¹ and the static structure factor of dense Kr gas at small wave vectors.¹²⁻¹⁴

Most predictions of the effect of the AT potential on the static and dynamic properties of rare gases stem from "exact" computer simulations (e.g., Monte Carlo or molecular-dynamics calculations) and include thermodynamic properties,^{15,16} pair correlation function,^{13,16-18} velocity autocorrelation function,^{16,19} and, to some extent, density fluctuations in dense gaseous Kr (Ref. 18), and liquid Ar (Ref. 16). In the present work we use the molecular-dynamics (MD) method to extend

these investigations to collective dynamical properties (transport coefficients, dynamical structure factor, and transverse current autocorrelation function) of Xe near its triple point. Xe was chosen for its large triple-dipole interaction and triple point conditions were chosen because experimental measurements of the transport coefficients were available.

In order to allow comparison with experiment a realistic pair potential for Xe was used. MD simulations were performed with this pair potential alone and with an added AT potential (for the sake of brevity we shall refer to these systems as two-body and three-body Xe, respectively). The results are compared both at constant-density-constant-temperature and at constant-pressure-constant-temperature conditions. The comparison was made as meaningful as possible by performing runs with identical statistics and particle numbers. As typically $(1-2) \times 10^5$ time steps are needed to obtain transport coefficients with a precision of 5-10% in the vicinity of the triple point, we restricted our system size to 108 particles to maintain computing time within acceptable length in the presence of three-body interactions. Details of the model and the MD simulations are given in Sec. II. In the following order we discuss the effect of the AT potential on the thermodynamic properties and pair correlation function (Sec. III), transport coefficients (Sec. IV), and dynamical structure factor and transverse current-current correlation function (Sec. V). A summary of the results is given in Sec. VI.

II. MODEL AND MD SIMULATIONS

The MD simulations were performed with either a pair potential alone or in combination with the AT potential

TABLE I. Effect of the Axilrod-Teller potential on internal energy U and compressibility factor Z . AS, B1, X2, and AT denote the pair potentials of Aziz and Slaman (Ref. 21), Lee *et al.* (Ref. 23), Barker *et al.* (Ref. 22), and the three-body Axilrod-Teller potential, respectively. Each independent run corresponds to 10000 time steps of 10^{-14} s. $Z^{(2)}$ is the pairwise additive and $Z^{(3)}$ the nonadditive contribution to Z . The statistical error on T is ± 0.3 K and on U is 0.002 kJ/mol.

System	Potential model	Number of independent runs	T (K)	ρ (mol/cm ³)	U (kJ/mol)	$Z = \frac{p}{\rho k_B T}$	$Z^{(2)}$	$Z^{(3)}$
A	AS + AT	10	176.4	0.0219	-10.83	0.23±0.02	-1.434	1.663
B	AS	10	175.9	0.0219	-11.65	-1.34±0.015		
C	AS	20	175.6	0.024	-12.77	0.16±0.015		
D	B1 + AT	5	173.1	0.0219	-10.64	0.16±0.04	-1.526	1.684
E	B1	15	174.5	0.0219	-11.47	-1.29±0.01		
F	X2	5	175.3	0.024	-12.75	0.16±0.04		
Expt. ^a			175	0.0219		~0		

^aReference 33.

$$V_3(\mathbf{r}_i, \mathbf{r}_j, \mathbf{r}_k) = \frac{\nu}{r_{ij}^3 r_{ik}^3 r_{jk}^3} \left[1 + \frac{3(\mathbf{r}_{ij} \cdot \mathbf{r}_{ik})(\mathbf{r}_{ji} \cdot \mathbf{r}_{jk})(\mathbf{r}_{ki} \cdot \mathbf{r}_{kj})}{r_{ij}^2 r_{ik}^2 r_{jk}^2} \right], \quad (1)$$

where $\mathbf{r}_{ij} = \mathbf{r}_j - \mathbf{r}_i$ is the separation between atoms i and j , $r_{ij} = |\mathbf{r}_{ij}|$, and $\nu = 749.8 \times 10^{-84}$ erg cm⁹ (Ref. 20) for Xe.

For the pair potential we primarily choose the HFD-B potential recently proposed by Aziz and Slaman²¹ (AS), which is consistent with a large variety of experimental information on pair interactions, including dilute gas properties, high-energy scattering data, dimer properties, etc. In addition, to estimate the influence of the pair potential on the thermodynamic and transport properties, computations were carried out for two pair potentials proposed earlier by Barker and co-workers, the X2 potential²² and the potential of Ref. 23 (which we will call B1). The well depths ϵ/k and distances of the potential minimum, r_m , are 282.29, 281, and 276 K and 4.3627, 4.3623, and 4.3655 Å for the AS, X2, and B1 potentials, respectively.

All simulations use 108 particles in a cubic volume with periodic boundary conditions. The pair potential was truncated at half the box length (~ 1 nm for the densities considered). For the three-body interactions only contributions from configurations for which the sides of the triangles formed by three particles are less than half the box length were considered to avoid ambiguities arising from the use of periodic boundary conditions. The equations of motion were solved using the Verlet algorithm²⁴ and the multiple-time-step method of Streett *et al.*;²⁵ the two-body forces were evaluated every $\Delta t = 10^{-14}$ s, whereas the more slowly varying AT three-body forces were calculated every $2\Delta t$ and extrapolated for intermediate times.

We considered six systems, labeled A–F in Table I, which differ by either the potential model or the density. The systems at density $\rho = 0.0219$ mol/cm³ and temperature $T \sim 175$ K correspond to a thermodynamic state close to the (experimental) triple point of Xe. Systems C and F at density $\rho = 0.024$ mol/cm³ have the same

compressibility factor $Z = p/\rho k_B T$ (p is the pressure and k_B is the Boltzmann constant) as system A and were designed to evaluate the effect of the AT potential at fixed pressure.

III. THERMODYNAMIC PROPERTIES AND PAIR CORRELATION FUNCTION

The internal energy U and compressibility factor Z for the different systems are compared in Table I. The contribution of the AT term to the internal energy is 7% of the two-body contribution and positive, indicating that contributions from triplets of particles forming acute triangles dominate. The effect on the compressibility factor is more pronounced and most clearly seen by splitting it into a part $Z^{(2)}$ involving only the pair potential v_2 (as well as the ideal-gas term) and a part $Z^{(3)}$ involving the AT potential v_3 . The two-body contribution $Z^{(2)}$ is negative and little affected by the AT potential (cf. systems A, B, D, E). It is largely canceled by $Z^{(3)}$, the net pressure being in close agreement with experiment, but not perfect. Similar good agreement has been shown by Barker³ to occur along the 423-K isotherm. Note that U and Z have been corrected for truncation of the two- and three-body potentials. The correction terms for $Z^{(2)}$ are -0.68 and -0.63 for states A and D, respectively. The correction for $Z^{(3)}$ has been estimated using the superposition approximation for the three-body correlation function¹⁵ and amounts to 0.096 for states A and D. Quantum corrections have been neglected as they are very small for Xe at the temperature considered.

Further evidence of the influence of the AT interaction on the pressure can be seen by comparing systems A and C or D and F (note that there is little difference between potentials B1 and X2). The results show that if the AT potential is turned off the density of the system has to be increased by as much as 10% in order to maintain a fixed pressure.

From the results of Table I it is apparent that in the liquid phase the systems of particles interacting by po-

tentials AS, B1, or X2 have nearly identical thermodynamic properties. This is seen to be true also if the AT potential is added to either of these pair potentials.

The small influence of the AT potential on the pair correlation function is illustrated by Fig. 1; this figure shows that the AT potential increases the pressure without reinforcing the local structure. This behavior confirms the possibility of a description of the AT interaction by a mean-field term, as recently suggested by Egelstaff.²⁶

IV. TRANSPORT PROPERTIES

In this section we present the results of our computations of the transport coefficients and compare them with experimental results for Xe. The three hydrodynamic transport coefficients, shear viscosity η_s , bulk viscosity η_v , and thermal conductivity λ were obtained from the Green-Kubo formulas²⁷

$$\eta_s = \int_0^\infty dt C_{\eta_s}(t), \quad (2a)$$

$$\eta_v = \int_0^\infty dt C_{\eta_v}(t), \quad (2b)$$

$$\lambda = \int_0^\infty dt C_\lambda(t). \quad (2c)$$

$C_{\eta_s}(t)$ and $C_{\eta_v}(t)$ are the autocorrelation functions of the off-diagonal and diagonal parts of the stress tensor,

respectively, and $C_\lambda(t)$ that of the heat flux density. These time correlation functions are equal to²⁷

$$C_{\eta_s}(t) = \frac{1}{3Vk_B T} \sum_{\substack{\alpha, \beta=1 \\ (\alpha < \beta)}}^3 \langle \sigma^{\alpha\beta}(0) \sigma^{\alpha\beta}(t) \rangle, \quad (3a)$$

$$C_{\eta_v}(t) = \frac{1}{9Vk_B T} \sum_{\alpha, \beta=1}^3 \langle [\sigma^{\alpha\alpha}(0) - \langle \sigma^{\alpha\alpha}(0) \rangle] \times [\sigma^{\beta\beta}(t) - \langle \sigma^{\beta\beta}(t) \rangle] \rangle, \quad (3b)$$

$$C_\lambda(t) = \frac{1}{3Vk_B T^2} \sum_{\alpha=1}^3 \langle J_e^\alpha(0) J_e^\alpha(t) \rangle, \quad (3c)$$

where V is the volume of the system.

The stress tensor is given by

$$\sigma^{\alpha\beta} = m \sum_i v_i^\alpha v_i^\beta - \frac{1}{2} \sum_{\substack{i, j \\ (i \neq j)}} \frac{\partial v_2}{\partial r_{ij}^\alpha} r_{ij}^\beta - \frac{1}{6} \sum_{\substack{i, j, k \\ (i \neq j \neq k)}} \left[\frac{\partial v_3}{\partial r_{ij}^\alpha} r_{ij}^\beta + \text{c.p.} \right], \quad (4)$$

and the heat flux by

$$J_e^\alpha = \sum_i E_i v_i^\alpha + \frac{1}{2} \sum_{\substack{i, j \\ (i \neq j)}} \left[\mathbf{v}_i \cdot \frac{\partial v_2}{\partial \mathbf{r}_i} \right] r_{ij}^\alpha + \frac{1}{9} \sum_{\substack{i, j, k \\ (i \neq j \neq k)}} \left[\left[\mathbf{v}_i \cdot \frac{\partial v_3}{\partial \mathbf{r}_i} \right] r_{ij}^\alpha + \text{c.p.} \right]. \quad (5)$$

m , \mathbf{v}_i , and E_i are the mass, velocity, and total energy of particle i , respectively,

$$E_i = \frac{1}{2} m \mathbf{v}_i^2 + \frac{1}{2} \sum_{\substack{j \\ (j \neq i)}} v_2(r_{ij}) + \frac{1}{6} \sum_{\substack{j, k \\ (i \neq j \neq k)}} v_3(\mathbf{r}_{ij}, \mathbf{r}_{ik}, \mathbf{r}_{jk}). \quad (6)$$

The normalized time correlation functions $C_\alpha(t)/C_\alpha(0)$ ($\alpha = \eta_s, \eta_v, \lambda$) for systems A–C are shown in Figs. 2–4. They correspond to averages over 10 (20 for system C) independent runs of 10 000 time steps, each with different initial conditions.

The most striking observation is that at a given density and temperature the effect of the AT potential is extremely small; the correlation functions for the AS and AS + AT potentials cannot be distinguished within statistical error, either in shape or in magnitude (cf. Table II where the initial values are collected). The decay of the various correlation functions is quite similar to that of a Lennard-Jones system near its triple point.^{28–31} In particular, the initial decay of C_{η_v} is somewhat faster than that of C_{η_s} and the amplitude of the “tail” at longer times slightly larger in C_{η_v} . However, the range of the long-time “tails” is essentially the same for both correlation functions. In view of the statistical error, estimated more precisely below, both correlation functions vanish within the range 2–3 ps.

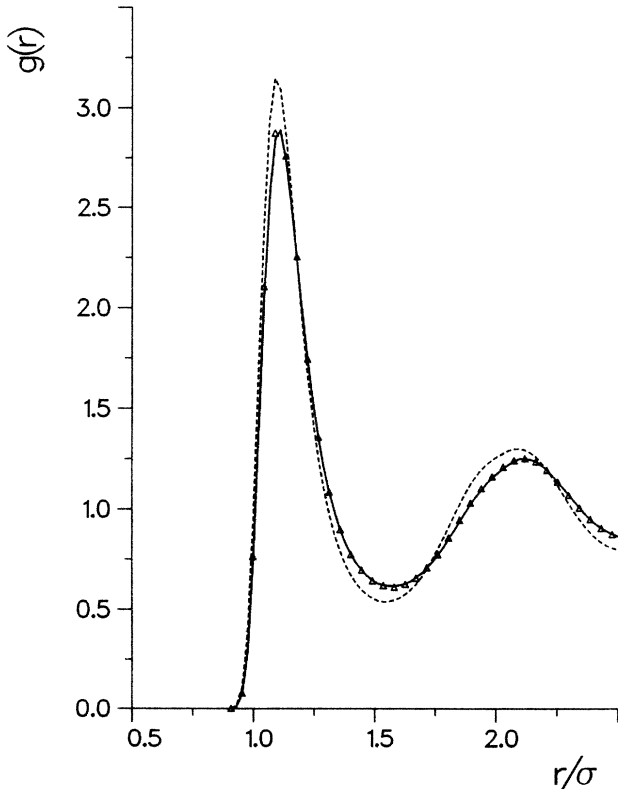


FIG. 1. Effect of the AT potential on the pair distribution function $g(r)$: Solid line, pair potential of Aziz and Slaman (AS) + Axilrod-Teller three-body potential at $\rho = 0.0219$ mol/cm³; triangles, AS potential, $\rho = 0.0219$ mol/cm³; dotted line, AS potential, $\rho = 0.024$ mol/cm³. ($\sigma = 3.8924$ Å.)

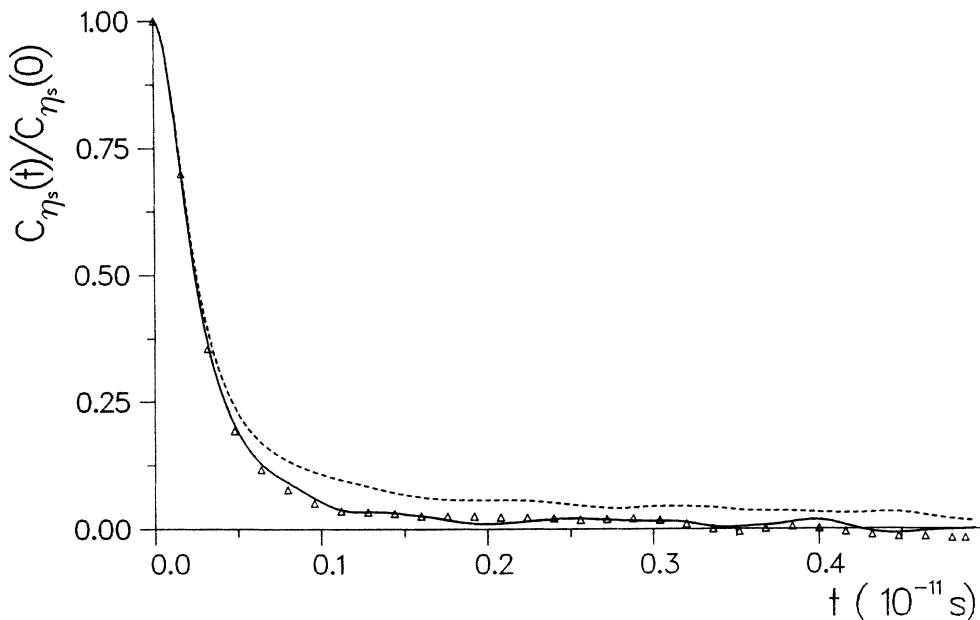


FIG. 2. Normalized time correlation function $C_{\eta_s}(t)/C_{\eta_s}(0)$ associated with the shear viscosity. The symbols are as in Fig. 1.

The correlation function $C_{\eta_v}(t)$ is more susceptible to statistical noise than $C_{\eta_s}(t)$ due to the necessity of subtracting the mean value of the diagonal part of the stress tensor [cf. Eq. (3b)]. In our calculations we subtracted for each value of t ,

$$\langle \sigma^{\alpha\alpha}(t) \rangle = \frac{1}{T-t} \sum_{\tau_i=\tau_0}^{T-t} \sigma^{\alpha\alpha}(t+\tau_i) \quad (7)$$

(where T is the maximum time span covered in the MD run) which guarantees that, for large t , $C_{\eta_v}(t) \rightarrow 0$. It is clear, however, that if, instead, the average pressure were subtracted, slightly different values would be obtained for C_{η_v} at large t .

If the time correlation functions associated with the transport coefficients corresponding to the AS and AS + AT potentials are compared *at constant pressure* (and constant temperature) the differences appear to be much larger (cf. systems A and C). Most spectacular is the enhancement, for the AS system, of the tail in $C_{\eta_s}(t)$ which extends to about 5 ps. The onset of long-lived tails in $C_{\eta_s}(t)$ and $C_{\eta_v}(t)$, typical of compressed or supercooled systems,³² is explained by the higher density of the AS system which is 10% higher than the triple point density of Xe, so that the system is very likely to be in a metastable state.

From Table II it is also apparent that upon compression of the AS system, the initial values $C_{\eta_s}(t=0)$ and

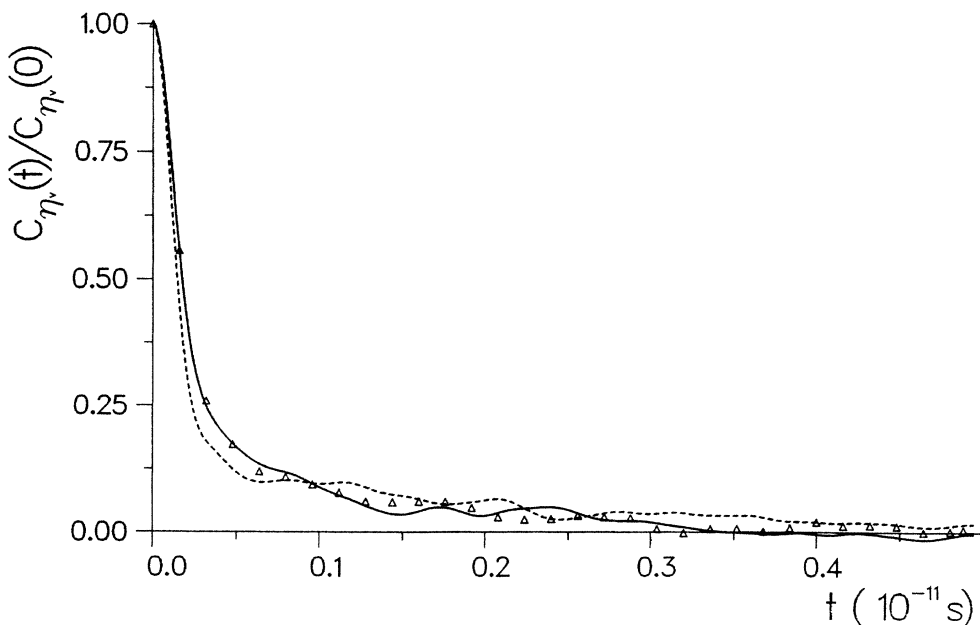


FIG. 3. Normalized time correlation function $C_{\eta_v}(t)/C_{\eta_v}(0)$ associated with the bulk viscosity. The symbols are as in Fig. 1.

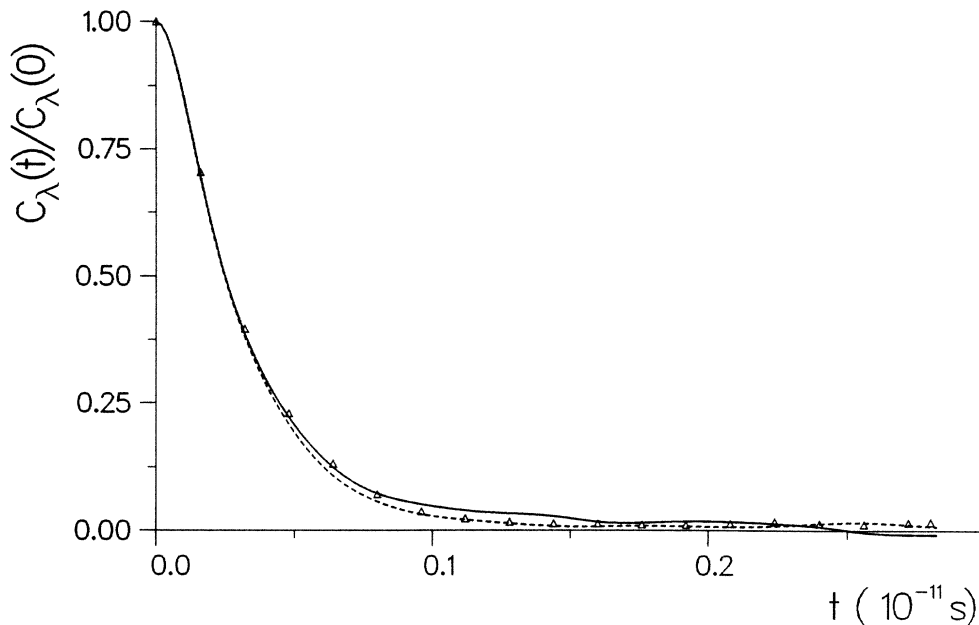


FIG. 4. Normalized time correlation function $C_\lambda(t)/C_\lambda(0)$ associated with the thermal conductivity. The symbols are as in Fig. 1.

$C_\lambda(t=0)$ increase, whereas $C_{\eta_v}(t=0)$ does not change significantly.

To estimate error bars for the time correlation functions and transport coefficients we considered two sources of error: the statistical error on the time correlation functions and the error due to the choice of an upper time limit in the integrals (2). The former was evaluated from the variance of the different independent runs and was found to be fairly independent of the value of time. Typical error bars based on one standard deviation are given in Table II for the initial values of the time correlation functions.

The time integrals in expressions (2) were truncated when the absolute magnitude of the average correlation functions became smaller than one standard deviation and the error bars on the transport coefficients are calculated from the variance of the values obtained for the different independent runs. These error bars (one standard deviation) are given in Table II. They amount to 5–10%. Similar estimates were obtained for a Lennard-Jones system³⁴ near triple point. For the density $\rho=0.0219$ mol/cm³ the truncation times were smaller (for C_λ) or of the order (for C_{η_s} and C_{η_v}) of the re-

currence time (time for an acoustic wave to travel across the simulation volume) which, for our 108-particle system, was estimated to be ~ 3.2 ps, using the experimental value for the sound velocity of Xe at 175 K (618 m/s).³³ For the compressed system $\rho=0.024$ mol/cm³ the truncation times for C_{η_s} and C_{η_v} exceeded the recurrence time adding error due to size effects on η_s and η_v . In view of this and the truncation of the time integrals the real uncertainties in the transport coefficients are presumably larger than the statistical error bars given in Table II.

On the basis of the similarity of the time correlation functions $C_\alpha(t)$ for two- and three-body Xe at constant density we do not expect any significant differences for the transport coefficients. This is readily checked from Table II. The results are also seen to be independent (within statistical error) of the form of the pair potential (AS or B1).

Upon compressing the AS system the shear viscosity increases due partly to the larger magnitude of the time correlation function and partly to its slower long-time decay. The bulk viscosity, on the contrary, is fairly insensitive to compression; although the long-time decay

TABLE II. Values of the transport coefficients and initial values of the associated time correlation functions for the various systems considered. Note that $C_{\eta_s}(t=0)$ and $C_{\eta_v}(t=0)$ are equal to the high-frequency shear and bulk moduli, C_∞ and K_∞ , respectively. The acronyms for the potential models are explained in Table I.

System	Potential	ρ (mol/cm ³)	$C_{\eta_s}(t=0)$ (10 ¹² mPa)	$C_{\eta_v}(t=0)$ (10 ¹² mPa)	$C_\lambda(t=0)$ (10 ¹⁶ erg K ⁻¹ cm ⁻¹)	η_s (mPa s)	η_v (mPa s)	λ (W K ⁻¹ m ⁻¹)
A	AS + AT	0.0219	1.09±0.02	0.82±0.02	1.90±0.05	0.41±0.03	0.31±0.04	0.068±0.004
B	AS	0.0219	1.08±0.02	0.79±0.02	1.89±0.03	0.40±0.03	0.30±0.03	0.064±0.003
C	AS	0.024	1.48±0.02	0.75±0.02	2.54±0.03	0.87±0.06	0.30±0.03	0.082±0.004
E	B1	0.0219	1.06±0.02	0.77±0.03	1.81±0.03	0.39±0.02	0.30±0.04	0.061±0.002
Expt. ^a		0.0219				0.45	0.208	0.0689

^aReference 33.

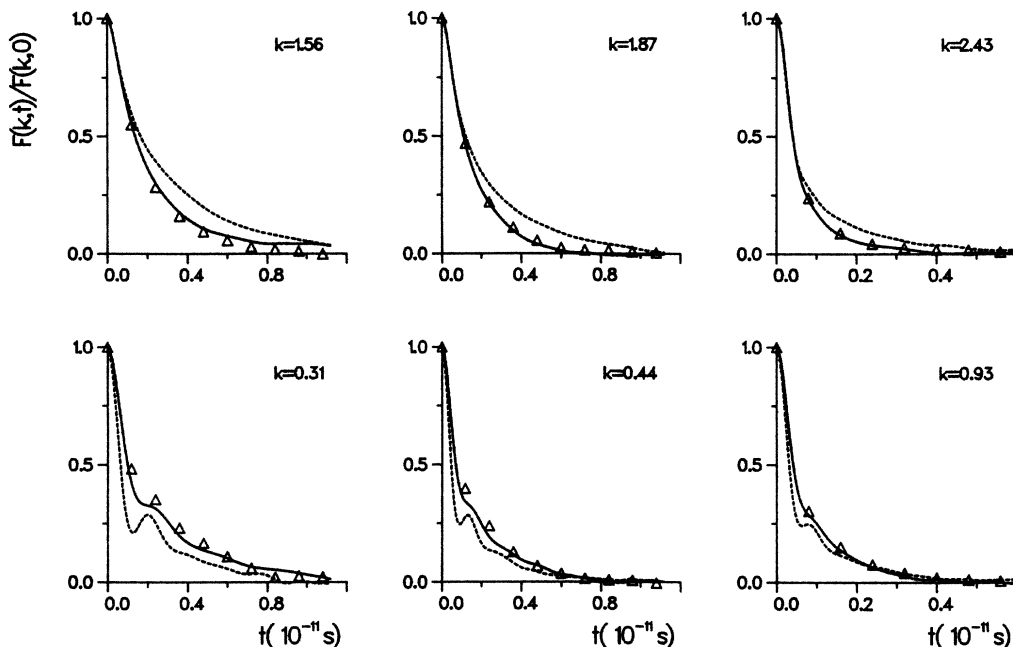


FIG. 5. Normalized intermediate scattering function $F(k,t)/F(k,0)$. The symbols are as in Fig. 1. The values of k (in \AA^{-1}) are those for the density $\rho=0.0219$ mol/cm³. The corresponding values for the system at $\rho=0.024$ mol/cm³ are $k=0.32, 0.45, 0.96, 1.61, 1.93,$ and 2.51 \AA^{-1} , respectively.

of C_{η_v} becomes slower the corresponding increase in η_v is compensated by a faster initial decay of the correlation function. Near constancy of η_v with density has also been observed in a recent study of supercooled soft spheres in the region outside formation of a glassy state.³² The thermal conductivity increases with density mainly due to the increase of $C_{\lambda}(t=0)$.

The calculated transport coefficients are compared

with experimental results by Malbrunot *et al.*³³ in Table II for the density $\rho=0.0219$ mol/cm³. At first sight it would appear that the calculated shear viscosity is too small. However, from previous simulations with the Lennard-Jones potential we know that a 108-particle system underestimates the shear viscosity by approximately 10% (compared to the infinite-particle limit) near the triple point due to a faster long-time decay of the corre-

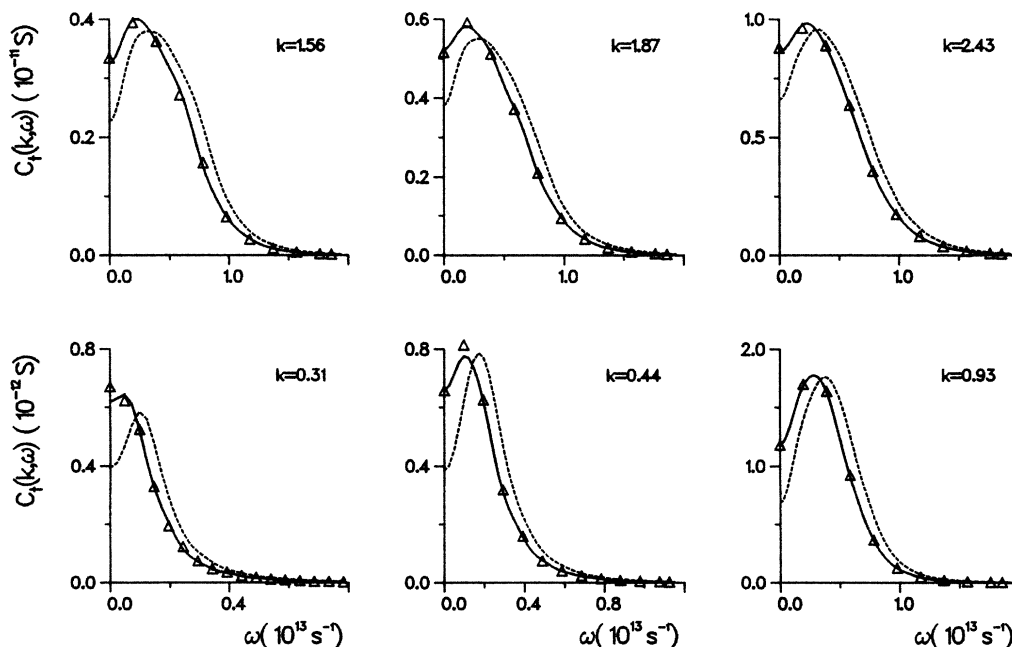


FIG. 6. Transverse current autocorrelation function. The symbols are as in Fig. 1. The values of k (in \AA^{-1}) are those for the density $\rho=0.0219$ mol/cm³. The corresponding values for the system at $\rho=0.024$ mol/cm³ are $k=0.32, 0.45, 0.96, 1.61, 1.93,$ and 2.51 \AA^{-1} , respectively.

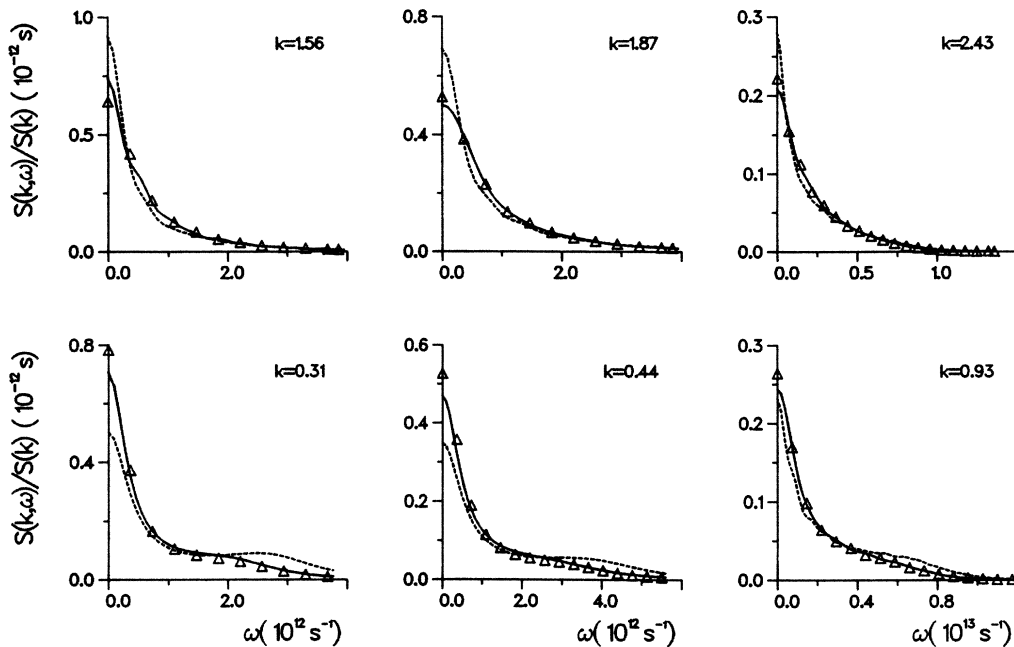


FIG. 7. Normalized dynamical structure factor $S(k, \omega)/S(k)$. The symbols are as in Fig. 1. The values of k (in \AA^{-1}) are those for the density $\rho=0.0219$ mol/cm³. The corresponding values for the system at $\rho=0.024$ mol/cm³ are $k=0.32, 0.45, 0.96, 1.61, 1.93,$ and 2.51 \AA^{-1} , respectively.

sponding time correlation functions.²⁹ If we correct our simulation value of η_s by this amount, satisfactory agreement is obtained with experiment.

The discrepancy observed for the bulk viscosity is much more pronounced and can hardly be explained by the combined uncertainties on both simulations and experiment. The latter may, however, be quite large (Malbrunot *et al.*³³ claim a maximum error of 25%) as a result of the fact that the bulk viscosity is measured only indirectly via the acoustic attenuation coefficient and requires prior knowledge of the shear viscosity, heat conductivity, and specific heats. Moreover, the variation of η_v with density is quite rapid in the vicinity of the triple point.³³ Finally we note that the thermal conductivity is in good agreement with experiment.

V. DYNAMICAL STRUCTURE FACTOR AND TRANSVERSE CURRENT AUTOCORRELATION FUNCTION

Further understanding of the influence of the AT potential on collective dynamical effects can be gained from the intermediate scattering function

$$F(k, t) = \frac{1}{N} \left\langle \sum_{i,j} e^{ik \cdot [r_i(0) - r_j(t)]} \right\rangle,$$

whose Fourier transform

$$S(k, \omega) = \frac{1}{2\pi} \int_{-\infty}^{\infty} F(k, t) e^{i\omega t} dt$$

is the dynamical structure factor measured in neutron scattering experiments and from the transverse current autocorrelation function

$$C_T(k, t) = \frac{1}{N} \left\langle \sum_{i,j} v_i^x v_j^x e^{ik \cdot [r_i(0) - r_j(t)]} \right\rangle,$$

the Fourier transform of which we denote $C_T(k, \omega)$, v_i^x is the component of the velocity of the i th particle perpendicular to k .

The wave vectors which have been studied, compatible with the periodic boundary conditions of the system, were $k=0.31, 0.44, 0.93, 1.56, 1.87,$ and 2.43 \AA^{-1} for density $\rho=0.0219$ mol/cm³ and $k=0.32, 0.45, 0.96, 1.61, 1.93,$ and 2.51 \AA^{-1} for $\rho=0.024$ mol/cm³.

The normalized intermediate scattering function $F(k, t)/F(k, t=0)$ and the Fourier transform $C_T(k, \omega)$ of the transverse current autocorrelation function for the AS and AS + AT potentials at density $\rho=0.0219$ mol/cm³ are compared in Figs. 5 and 6. The differences are small and statistically significant only for $F(k, t)$ for the two lowest k values considered: At these wave vectors $F(k, t)$ is slightly narrower for the three-body system, giving rise to a somewhat lower value of $S(k, \omega)$ at low frequency (cf. Fig. 7). We also remark that for small k the initial value of $F(k, t)$ which is equal to the static structure factor $S(k)$ is reduced by the AT potential (cf. Table III). This is compatible with a smaller value of the compressibility [$k \rightarrow 0$ limit of $S(k)$]. However, these differences appear more distinctly if we do a comparison at constant pressure. In $F(k, t)$ they manifest themselves, for the AS potential, by a smaller damping of sound waves at small k , which induces a somewhat more pronounced high-frequency "shoulder" in $S(k, \omega)$ (cf. Fig. 7). These features are consistent with the higher density of the AS system. From $C_T(k, \omega)$ we further conclude that for this higher density the propagation of shear modes persists to much larger wavelengths. A propagating mode is still observed for the lowest k vec-

TABLE III. Initial value of the intermediate scattering function: $F(k, t=0)=S(k)$. Note that systems A and B have density $\rho=0.0219$ mol/cm³ and system C, $\rho=0.024$ mol/cm³.

$k\sigma$	System A AS + AT	System B AS	System C AS
1.21	0.059±0.004	0.068±0.003	
1.25			0.032±0.001
1.71	0.060±0.003	0.066±0.002	
1.77			0.035±0.001
3.64	0.098±0.002	0.098±0.002	
3.75			0.067±0.001
6.06	1.43±0.05	1.41±0.06	
6.25			1.50±0.05
7.27	1.63±0.03	1.60±0.05	
7.50			1.52±0.05
9.47	0.64±0.01	0.64±0.01	
9.76			0.61±0.01

tor considered, whereas for the triple point density this value is close to the one at which shear modes disappear.

VI. SUMMARY

We have investigated by MD simulations the influence of the AT three-body potential on the collective properties, especially the transport coefficients of Xe near the triple point. Our principal finding is that for fixed density and temperature the AT potential primarily affects the thermodynamic properties of the system (pressure, compressibility) giving good agreement with experiment and affects only in a very minor way the collective dynamical properties which we have considered. In particular, the transport coefficients, shear, bulk viscosities, and thermal conductivity, near triple point are found to be insensitive (within statistical error) to the presence of the AT potential and also to the precise form chosen for the two-body potential. These findings corroborate the mean-field picture of many-body forces recently put forward by Egelstaff.²⁶ The AT potential does not seem to appreciably affect fluctuations in the system and consequently will not alter the values for the transport coefficients.

The preceding comparisons pertain to a system of 108 particles. Due to the small contribution of the three-body forces to the transport coefficients, possible finite-size corrections will affect primarily the contribution from the two-body forces. These corrections have been published previously.^{29-31,34,35} From the work of Hoheisel and collaborators on the Lennard-Jones system near triple point²⁹⁻³¹ it would appear that only the shear viscosity is significantly affected by a 108-particle system (10%, as mentioned in Sec. IV). After correction for this finite-size effect, the shear viscosity is in satisfactory

agreement with experiment. The thermal conductivity, which is rather insensitive to the particle number, also agrees well with experiment. However, a discrepancy seems to occur for the bulk viscosity, the origin of which is not yet clearly understood.

The effect of the AT potential on $S(k, \omega)$ is also small and statistically significant only at low frequency and low wave vectors. Unfortunately, in the absence of neutron scattering measurements of $S(k, \omega)$ in Xe near the triple point we have no estimate of the global contribution of many-body forces to $S(k, \omega)$. Egelstaff and co-workers,³⁶ by comparing neutron scattering data of $S(k, \omega)$ for room-temperature Kr gas at about twice the critical density with simulation results using the best available pair potential found a marked effect of many-body forces on $S(k, \omega)$ in the range $0.6 \text{ \AA}^{-1} < k < 1.3 \text{ \AA}^{-1}$. Unless the role of the AT potential is much enhanced for this thermodynamic state, the present study would indicate that this effect cannot be explained by the AT potential only. Computer simulations recently undertaken for Kr gas confirm this result.³⁷

When comparing the properties of two- and three-body Xe at constant pressure we come up against the difficulty that the thermodynamic state corresponding to the two-body potential is in a metastable region due to the rather large increase in density (10% of the triple point density) which is required to reproduce the pressure of the three-body system. As a consequence, a direct comparison of the properties of the two states belonging to different phases may not be very meaningful. This difficulty arises, of course, due to our proximity to the triple point. In any case, the compressed system (AS potential) is shown to have a larger shear viscosity and thermal conductivity. Also, sound waves are less damped and propagating shear waves persist to larger wavelengths.

Note that at the density 0.0219 mol/cm³ the pure two-body system is also metastable (negative pressure). However, the difference in pressure between the two- and three-body systems does not seem to entail significant differences in the collective dynamical properties.

We finally remark that the present study occurs in the framework of the weakly polarizable rare gases. For strongly polarizable systems, such as water, the effect of the three-body forces on collective dynamics has been shown to be much more important.³⁸

ACKNOWLEDGMENTS

Part of the calculations were performed on the Cray-1S computer at Ecole Polytechnique (Palaiseau). We thank the Conseil Scientifique of the Centre de Calcul Vectoriel pour la Recherche for allocation of the computer time. Laboratoire de Physique Théorique et Hautes Energies is "Laboratoire associé au Centre National de la Recherche Scientifique."

- ¹See, for example, J. A. Barker, in *Rare Gas Solids*, edited by M. L. Klein and J. A. Venables (Academic, New York, 1976), Vol. 1, Chap. 4.
- ²J. A. Barker, *Mol. Phys.* **57**, 755 (1986).
- ³J. A. Barker, *Phys. Rev. Lett.* **57**, 230 (1986).
- ⁴W. J. Meath and R. A. Aziz, *Mol. Phys.* **52**, 225 (1984).
- ⁵E. E. Polymeropoulos, J. Brickmann, L. Jansen, and R. Block, *Phys. Rev. A* **30**, 1593 (1984).
- ⁶B. H. Wells and S. Wilson, *Mol. Phys.* **55**, 199 (1985).
- ⁷M. Bulski and G. Chalansinski, *Chem. Phys. Lett.* **89**, 450 (1982).
- ⁸J. A. Barker, *Mol. Phys.* **60**, 887 (1987).
- ⁹J. A. Barker, *J. Chem. Phys.* (to be published).
- ¹⁰P. Loubeyre, *Phys. Rev. Lett.* **58**, 1857 (1987); and (unpublished).
- ¹¹E. E. Polymeropoulos, P. Bopp, J. Brickmann, L. Jansen, and R. Block, *Phys. Rev. A* **31**, 3565 (1985).
- ¹²A. Teitsma and P. A. Egelstaff, *Phys. Rev. A* **21**, 367 (1980).
- ¹³P. A. Egelstaff, A. Teitsma, and S. S. Wang, *Phys. Rev. A* **22**, 1702 (1980).
- ¹⁴P. A. Egelstaff, W. Glaser, D. Litchinsky, E. Schneider, and J. B. Suck, *Phys. Rev. A* **27**, 1106 (1983).
- ¹⁵J. A. Barker, R. A. Fisher, and R. O. Watts, *Mol. Phys.* **21**, 657 (1971).
- ¹⁶C. Hoheisel, *Phys. Rev. A* **23**, 1998 (1981).
- ¹⁷J. M. Haile, in *Computer Modeling of Matter*, edited by P. Lykos (Am. Chem. Soc., Washington, D.C., 1978), p. 172.
- ¹⁸W. Schommers, *Phys. Rev. A* **22**, 2855 (1980).
- ¹⁹W. Schommers, *Phys. Rev. A* **27**, 2241 (1983).
- ²⁰R. J. Bell and A. E. Kingston, *Proc. Phys. Soc.* **88**, 901 (1966).
- ²¹R. A. Aziz and M. J. Slaman, *Mol. Phys.* **57**, 825 (1986).
- ²²J. A. Barker, R. O. Watts, J. K. Lee, T. P. Schafer, and Y. T. Lee, *J. Chem. Phys.* **61**, 3081 (1974).
- ²³J. K. Lee, D. Henderson, and J. A. Barker, *Mol. Phys.* **29**, 429 (1975).
- ²⁴L. Verlet, *Phys. Rev.* **159**, 98 (1967).
- ²⁵W. B. Streett, D. J. Tildesley, and G. Saville, *Mol. Phys.* **35**, 639 (1978).
- ²⁶P. A. Egelstaff, *Europhys. Lett.* **3**, 867 (1987).
- ²⁷R. W. Zwanzig, *Ann. Rev. Phys. Chem.* **16**, 67 (1965).
- ²⁸D. Levesque, L. Verlet, and J. K urkijarvi, *Phys. Rev. A* **7**, 1690 (1973).
- ²⁹M. Schoen and C. Hoheisel, *Mol. Phys.* **56**, 653 (1985).
- ³⁰C. Hoheisel, *J. Chem. Phys.* **86**, 2328 (1987).
- ³¹R. Vogelsang, C. Hoheisel, and G. Cicotti, *J. Chem. Phys.* **86**, 6371 (1987).
- ³²J. G. Amar and R. D. Mountain, *J. Chem. Phys.* **86**, 2236 (1987).
- ³³P. Malbrunot, A. Boyer, E. Charles, and H. Abachi, *Phys. Rev. A* **27**, 1523 (1983).
- ³⁴D. Levesque and L. Verlet, *Mol. Phys.* **61**, 143 (1987).
- ³⁵J. J. Erpenbeck and W. W. Wood, *J. Stat. Phys.* **24**, 455 (1981).
- ³⁶J. J. Salacuse, W. Schommers, and P. A. Egelstaff, *Phys. Rev. A* **34**, 1516 (1986).
- ³⁷D. Levesque and J. J. Weis (unpublished).
- ³⁸M. Wojcik and E. Clementi, *J. Chem. Phys.* **85**, 3544 (1986); **85**, 6085 (1986).